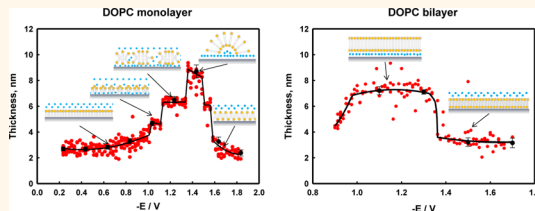


# Direct Characterization of Fluid Lipid Assemblies on Mercury in Electric Fields

Alexander Vakurov,<sup>†,\*</sup> Massimiliano Galluzzi,<sup>†</sup> Alessandro Podestà,<sup>†</sup> Nikita Gamper,<sup>‡</sup> Andrew L. Nelson,<sup>†</sup> and Simon D. A. Connell<sup>§</sup>

<sup>†</sup>School of Chemistry, University of Leeds, Leeds, LS2 9JT, U.K., <sup>‡</sup>School of Biology, University of Leeds, Leeds, LS2 9JT, U.K., <sup>§</sup>School of Physics and Astronomy, University of Leeds, Leeds, LS2 9JT, U.K., and <sup>†</sup>C.I.MA.I.Na and Department of Physics, Università degli Studi di Milano, Via Celoria 16, 20133 Milano, Italy

**ABSTRACT** Phospholipid monolayers on mercury (Hg) surfaces have received substantial and extensive scientific interest not only because of their use as a biomembrane model but also for their application as a successful toxicity-sensing element. The monolayers show characteristic and very reproducible phase transitions manifest as consecutive voltammetric peaks in response to applied transverse electric fields. Unfortunately, apart from the results of simulation studies, there is a lack of data on the lipid phase structures to help interpret these voltammetric peaks. In this paper we report on the direct measurement of the structural changes underlying the phase transitions of phospholipid layers of dioleoyl phosphatidylcholine (DOPC) at electrified Hg surfaces using atomic force microscopy force–distance techniques. These direct measurements enable a description of the following structural changes in fluid lipid assemblies on a liquid electrode within an increasing transverse electric field. At about  $-1.0$  V (vs Ag/AgCl) a field-facilitated ingress of ions and water into the monolayer results in a phase transition to a structured 2D emulsion. This is followed by a further phase transition at more negative potentials involving the readorption of bilayer patches. At stronger values of field the bilayer patches form semivesicles, which subsequently collapse to form a monolayer of uncertain composition at very negative potentials. The observation that a monolayer on Hg converts to a bilayer by increasing the applied potential has allowed techniques to be developed for preparing and characterizing a near-continuous DOPC bilayer on Hg in an applied potential window within  $-1.0$  and  $-1.4$  V (vs Ag/AgCl).



**KEYWORDS:** phospholipid · DOPC · fluid lipid · mercury surface · electric field · phase transitions · monolayer/bilayer · atomic force microscopy (AFM)

**S**upported phospholipid bilayers and supported phospholipid monolayers<sup>1–7</sup> on substrates such as gold<sup>8–19</sup> are widely used model systems for the study of biomembrane function. They are also applied to the development of biosensors where the biomembrane in some form acts as a sensing element. Within the domain of supported lipid layers, liquid metal compared with solid metal supports has unique advantages since the liquid metal surface has a low surface roughness that is difficult to approach on solid gold substrates. Because of this, fluid phospholipid, usually dioleoyl phosphatidylcholine (DOPC), coated mercury (Hg) electrodes have been studied and applied extensively.<sup>20–47</sup> Indeed the fluid phospholipid monolayer on Hg has been seen as the classical electrochemical biomembrane model used as a system for developing fundamental

theories concerning phase behavior of phospholipids and water in electric field<sup>31,33,35</sup> and channel transport of ions.<sup>36,37</sup> In spite of the interest in the Hg phospholipid system, the formation of the monolayer on Hg has generally been investigated only using electrochemical and simulation techniques, and the monolayer configuration and its behavior in transverse electric fields have never been unequivocally characterized by direct physicochemical methods. Originally, hanging mercury drop electrodes (HMDE) were used for characterizing phospholipid layers on Hg. Such electrodes are fragile, have uncertain long-term stability, and contain macroscopic amounts of Hg, making them difficult to access with microscopic techniques. A study<sup>28,29</sup> has been carried out using epifluorescence microscopy to attempt to image the behavior of DOPC in varying fields on the HMDE. Some

\* Address correspondence to a.vakurov@leeds.ac.uk.

Received for review July 19, 2013 and accepted March 13, 2014.

Published online March 13, 2014  
10.1021/nn4037267

© 2014 American Chemical Society

interesting results were obtained, but problems were encountered through quenching of the fluorescence by the Hg surface. In addition the investigation necessitated the long-term stability of the same Hg drop attached to an HMDE capillary, which was particularly challenging. Another recent investigation used scanning electrochemical microscopy (SECM) to monitor ion transport through gramicidin channels in the Hg-phospholipid system using a gramicidin-DOPC-coated Tl amalgam HMDE as emitter and a Pt/Hg ultramicroelectrode as detector.<sup>38</sup> Although the study confirmed the selective transport of Tl(I) through the gramicidin channel, the SECM technique provided no direct physical information on the structure of the layers. Recently wafer-based Hg film electrodes have been fabricated,<sup>39,40</sup> which are very much more robust than the HMDE and unlike the HMDE can readily be accessed by spectroscopic and microscopic examination. In addition the wafer-based Hg electrodes support fluid phospholipid layers with identical electrochemical properties to those supported on an HMDE.<sup>39,40</sup>

The electrode miniaturization improves the accessibility of the Hg-lipid model to experimentation, but one drawback of the approach is that up until now the model consists of only a phospholipid monolayer and not a bilayer on Hg. This means that the model is not completely relevant to the biomembrane, which has a bilayer backbone. Only a direct physicochemical investigation would enable conditions to be varied to enable the possible formation and confirmation of phospholipid bilayer structures on Hg. If this development were possible, it would open up new and important applications for this very versatile experimental system. The work described below has been an attempt to advance the field in this direction.

Rapid cyclic voltammetry (RCV) of the fluid phospholipid coated Hg shows consecutive capacitance current peaks concurrent with consecutive phase transitions, respectively,<sup>39,40</sup> which are characteristic for each specific phospholipid. These phase transitions correspond to a poration and eventual "breakdown" of the layers and have long been seen to be a realistic model of electroporation processes in bilayers and biomembranes.<sup>31</sup> In addition the mechanisms behind the transitions involve very subtle changes in the intermolecular forces between the lipid molecules and the lipid molecules and water, which are altered by the transverse electric field.<sup>33</sup> These processes therefore are fundamental to the properties of phospholipid self-assembly directed by field. The uniqueness of the system of fluid lipids on Hg is shown by the fact that the sharp discontinuous phase transitions are not observed with fluid phospholipids on solid metals or with phospholipids below their phase transition temperature.<sup>13–15</sup> The reason for this is that the sharpness of the phase transitions depends on the highly ordered structure of the monolayer, which reflects the

compatibility of the fluid DOPC with the liquid Hg surface. Solid metals even in their single-crystal<sup>48</sup> or template-stripped<sup>49</sup> configuration have terraces and an atomic-scale roughness, respectively, on the surface, which prevents the supported lipid from having a continuous perfectly smooth ordered structure. At the same time solid metals undergo surface reconstruction when their potential is altered,<sup>50</sup> leading to the formation of additional defects and terraces, which will influence the supported lipid order in addition to effects mediated through the alteration in potential alone. With respect to the properties of nonfluid lipid layers on liquid metals, lipid monolayers below their solid–liquid phase transition temperature exhibit grain boundaries in their structure.<sup>51</sup> The existence of these grain boundaries undermines the order of the monolayer as well as permeabilizing the monolayer to water and ions. These effects will degrade the discontinuity of potential-induced phase transitions, as has been observed with monolayers of dipalmitoyl phosphatidylcholine (DPPC) on Hg.<sup>21</sup>

It is therefore apparent that the sharp potential-induced discontinuities of structure of the fluid lipid layers on Hg are specific to the system; however the interpretation of the mechanistic details of the potential-induced phase transitions has not been without controversy. Miller<sup>19</sup> originally indicated that the voltammetric peaks at very negative potentials represented a desorption of the phospholipid from the Hg; however Nelson's original studies<sup>21,22</sup> on the HMDE seemed to show that the adsorbed phospholipid layers were more stable than previously assumed. In Nelson's study all voltammetric peaks were allocated to reorientation and layer breakdown processes, although later epifluorescence<sup>28,29</sup> and impedance studies<sup>41</sup> have presumed the phospholipid desorbs at very negative potentials. In addition, an alternative simulation model quantitatively related the voltammetric peaks to a rotation of the lipid molecules in response to field on the Hg surface.<sup>42</sup> In spite of this the uncertainty regarding the "reorientation" voltammetric peaks of the lipid layer in field has prevailed. Currently, the general consensus on the structural changes with increasing field of DOPC layers on Hg is that (a) the first capacitance current peak (−0.95 to −1.0 V) is concurrent with the permeation of the layer to ions<sup>31,32</sup> and the layer's desorption from<sup>31</sup> the electrode surface, (b) the second capacitance current peak (−1.1 V) represents a nucleation and growth process of bilayer patches readsorbing onto the electrode surface,<sup>27,32,33,35</sup> and (c) the third capacitance current peak (−1.35 V) or groups of capacitance current peaks indicate the desorption of the phospholipid from the Hg surface.<sup>27,29</sup> It is considered that the electrode at more negative potentials than −1.7 V is essentially uncoated, although the phospholipid may lie in close vicinity to it.<sup>27,28</sup> The objective of this paper therefore is to establish the

precise validity of these previous assumptions regarding the behavior of phospholipid layers in electric field using direct microscopic measurements on the fluid phospholipid, DOPC, deposited on the wafer-based Hg film electrodes. Atomic force microscopy (AFM) was used to determine a comprehensive replicate series of force–distance curves at closely spaced, varied applied potentials. AFM has been previously deployed for the study of the structure and properties of phospholipid bilayers on Au(111)<sup>17–19</sup> in an electric field. On the other hand AFM has never before been applied to similar investigations of phospholipid mono/bilayers on Hg. The AFM force–distance measurements give layer thickness, resistance to AFM tip penetration, and coverage data as a function of potential. The AFM experimental data have enabled the physical changes that underlie the electric field driven phase transitions of DOPC phospholipid layers on Hg electrodes to be characterized. Another objective of this paper is to exploit a direct physicochemical characterization of the layers to design a technique to deposit continuous or near-continuous phospholipid bilayers on the electrode surface.

## RESULTS AND DISCUSSION

AFM measurements were begun at an applied potential of  $-0.4$  V since  $-0.4$  V is close to the PZC of Hg<sup>27</sup>

and is the point where monolayers of DOPC on Hg are homogeneous and impermeable to ions.<sup>25,27</sup> Analysis of AFM force–distance curves of the DOPC monolayer coated Hg at  $-0.4$  V shows a clear step of  $2.5\text{--}3$  nm (see Figure 1). The thickness of a hydrophobic core of a DOPC bilayer is given as  $\sim 3$  nm.<sup>52,53</sup> The size of the headgroup and bonded water increases this thickness to  $\sim 5\text{--}6$  nm.<sup>54–57</sup> The thickness of a monolayer is half that of a bilayer; thus a monolayer has a thickness of  $2.5\text{--}3$  nm. Consequently the evidence indicates that the DOPC forms a monolayer on a Hg surface at  $-0.4$  V applied potential. In contrast, the uncoated Hg did not show any steps at any voltages (data not shown). RCVs were taken prior to the AFM experiment and indicated the presence of a DOPC monolayer on the Hg with characteristic capacitance current peaks representing sequential phase transitions (Figure 2a).

Figure 3a shows the profile of the DOPC lipid layer thickness as a function of applied potential. It is observed that a perfect monolayer of 100% coverage increases in thickness from  $2.5$  nm to  $3.5$  nm over potentials from  $-0.2$  V to about  $-1$  V. This thickness increase is commensurate with previous simulations of the permeation of aquated ions through the layer accumulating on the electrode surface.<sup>31</sup> Lipkowski's group also found that a dimyristoyl PC (DMPC) bilayer

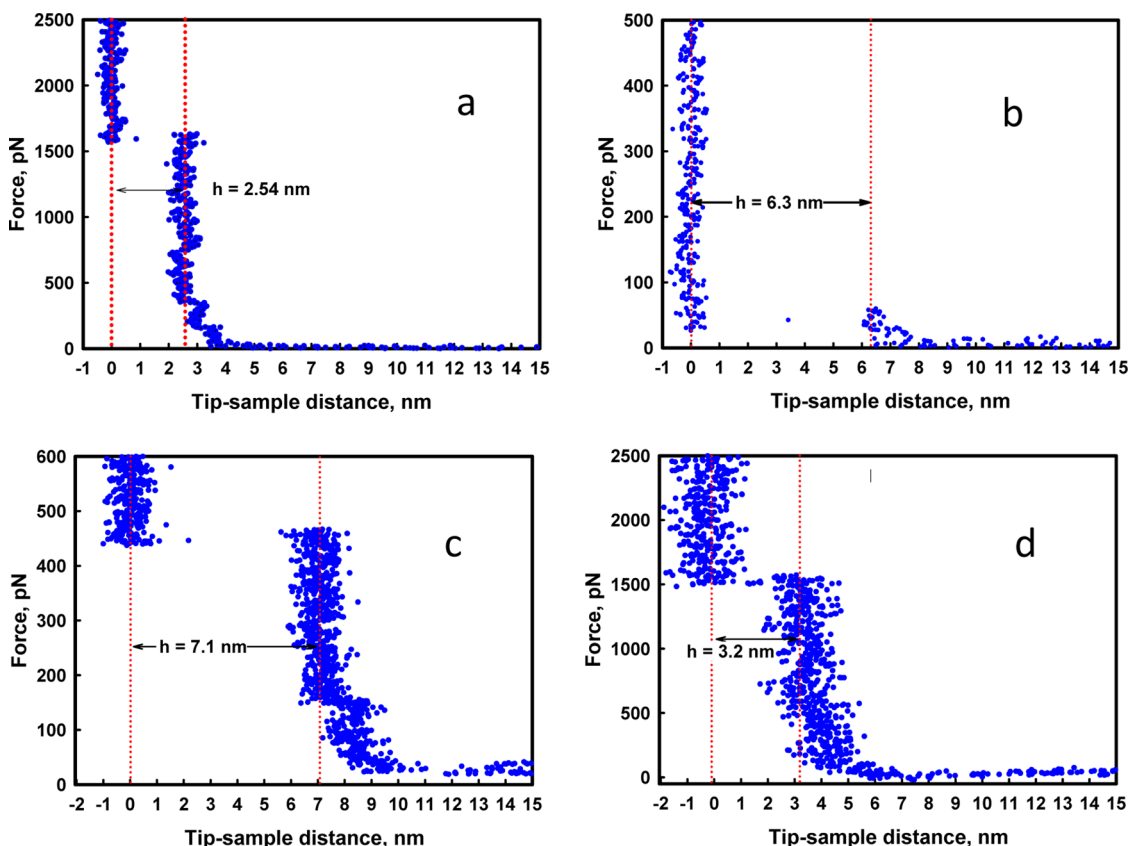
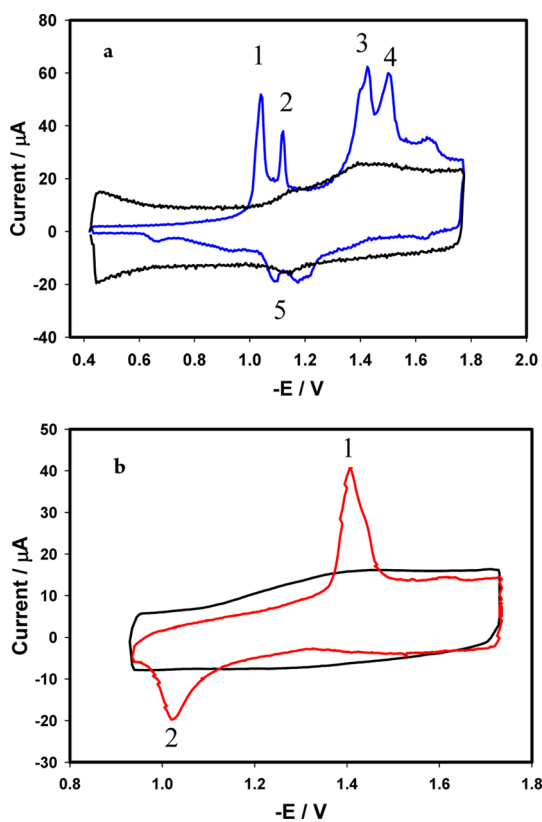
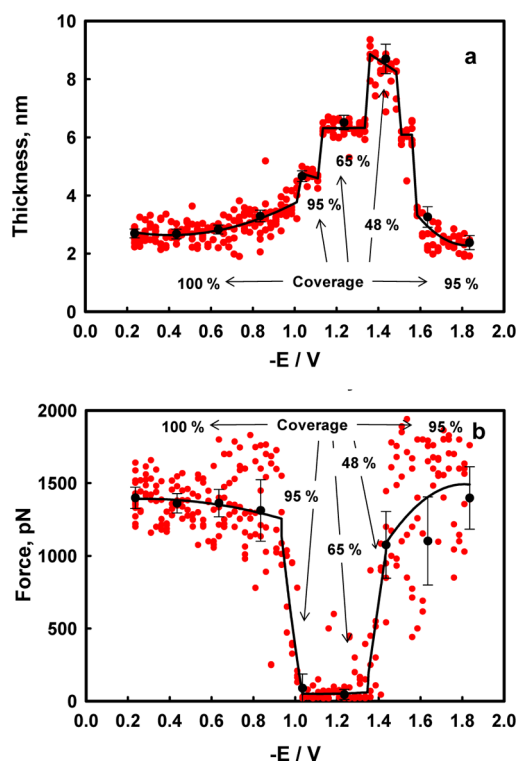


Figure 1. Characteristic AFM force–distance curves of a DOPC monolayer on Hg at  $-0.4$  V (a) and  $-1.2$  V (b) and a DOPC bilayer at  $-1.2$  V (c) and  $-1.8$  V (d).



**Figure 2.** Rapid cyclic voltammetry (RCV) of DOPC (a) monolayer (blue line) and (b) presumed bilayer (red line) on a Hg film electrode during AFM experiments. Black line denotes RCV of uncoated Hg. Peaks 1–5 in monolayer RCV and peaks 1 and 2 in bilayer RCV correspond to conformational changes in the DOPC mono- and bilayer. Each scan represents RCV in steady-state conditions.

on a gold electrode at negative potentials increases the effective thickness of the bilayer by up to 1.1 nm due to water and ionic accumulation between the gold surface and the dimyristoyl PC bilayer.<sup>13,14</sup> In the experiments reported in this study an increase of 1 nm was observed, which is similar to that found by Lipkowski's group. At about  $-1.02$  V a sharp increase in thickness is observed from 3.6 nm to 4.7 nm, which is close to a bilayer thickness. However a subtraction of a layer thickness of aquated ions would decrease the thickness of the layer to 3.7 nm, which is less than that of a bilayer and greater than that of a compact monolayer. The monolayer penetration force with the AFM tip (Figure 3b) decreases dramatically at the same potential. This indicates that the DOPC monolayer becomes softer or more exactly acquires a very much decreased stiffness, lateral density, and strength in self-assembly hydrophobic forces. The results concur with previous electrochemical measurements where at  $-1.02$  V the monolayer's permeability to cations increases dramatically accompanied by an increase in the monolayer capacitance.<sup>27</sup> Accordingly the sharp increase in thickness corresponds to an ingress of aquated ions into the monolayer to build up a double-layer structure on the Hg electrode surface with consequent monolayer



**Figure 3.** Coverage, (a) thickness, and (b) tip penetration force of a DOPC monolayer on a Hg film electrode vs applied potential as measured by AFM.

desorption and rearrangement.<sup>31</sup> In addition the softening of the DOPC layer and a decrease in coverage from 100% to 95% correlate with previous speculations indicating the formation of some kind of ordered water/phospholipid emulsion<sup>32</sup> of a 2D lipid sponge structure<sup>58</sup> or a half monolayer/half bilayer type structure.<sup>33</sup> The potential coincident with this process is that characterizing the first capacitance current peak on the RCV (peak 1 in Figure 2a).

A further increase in thickness to 6.3 nm is observed at  $-1.12$  V; 6.3 nm is approximately the thickness of a DOPC bilayer including the water and ions associated with the adsorbed DOPC head groups. The coverage of 65% indicates that the electrode is only partly covered by the bilayer or the bilayer exists as bilayer patches. The sharp increase in thickness is exactly coincident with the potential characterizing the onset of the second capacitance current peak on the RCV (peak 2 in Figure 2a). This result is commensurate with the previous simulation that the second capacitance current peak corresponded to the formation of bilayer patches.<sup>33</sup> The nucleation and growth<sup>27,32</sup> mechanism that underlies this process leads to the readsorption of bilayer patches on the electrode surface. In fact the readsorption of bilayer patches is evidenced from the chronoamperometric current transients that characterize the phase transition. A current transient can signify only a displacement of charge on the Hg surface, which concurs with the adsorption of the charged DOPC heads<sup>34</sup> in place of electrolyte counterions.

A third jump in thickness occurs at applied potentials of about  $-1.35$  V. The thickness increases to about  $8.3$  nm and the coverage decreases to  $48\%$ . The thickness of  $8.3$  nm does not correspond to a vesicle, which would be at the very least two bilayers thick, but it could represent a partial desorption of a bilayer, leading to semivesicular structures attached to the electrode. This is in agreement with the lower force for penetration and decreased coverage.

At  $-1.5$  V, the layer thickness collapses *via* a step of  $6$  nm to  $2.5$ – $3$  nm, which remains constant at more negative potentials. The force for penetration increases correspondingly to that of the monolayer at  $-0.4$  V. The layer is stable with a coverage increasing to  $95\%$ . The layer thickness of  $2.5$ – $3$  nm is equivalent to a monolayer thickness. This is not an expected result since a desorption of the monolayer at these potentials has been previously assumed.<sup>27,28</sup> Close examination of Bizzotto's work on epifluorescence<sup>28,29</sup> shows a quenching of fluorescence of labeled DOPC at very negative potentials of about  $-1.75$  V. This indicates the adsorbed DOPC is in close proximity to the Hg surface, inferring a compressed monolayer structure at this potential. This result has to be reconciled with the capacitance of the DOPC-covered Hg electrode at this potential, which is identical to that of uncoated Hg. It can only be assumed that at the high values of electric field a compact layer of counterions is maintained on the electrode surface with the compressed DOPC layer on top. Lipkowski's group found a bilayer structure of DMPC to exist on a gold electrode at similar rational negative potentials to those applied in this study, and no desorption was observed.<sup>13,14</sup>

From the results describing the DOPC monolayer behavior on Hg in an electric field, it can be presumed that there is a potential window between  $-1.0$  and  $-1.4$  V where a complete DOPC bilayer could exist on the Pt/Hg. As a consequence, after a number of experiments an RCV scan of voltage excursion  $-1.1$  to  $-3.0$  V was chosen as the most effective to facilitate continuous (not patched) bilayer deposition with the electrode exposed to DOPC vesicle dispersion.

To monitor the presumed bilayer formed in this way, an RCV scan was applied with voltage excursion from  $-1.7$  to  $-0.9$  V. The resulting RCV profile consisted of one large capacitance current peak at about  $-1.4$  V on the cathodic scan, which was apparently reversed on the anodic scan as a smaller peak at  $-1.0$  V (peaks 1 and 2, respectively, in Figure 2b). Significantly, the potential of this peak 1 on the cathodic scan was similar to the potential that characterized the third capacitance current peaks 3 and 4 of a DOPC monolayer on Hg. AFM data (see Figure 4a) show that at potentials between  $-1.7$  and  $-1.35$  V the structure of this assembly has the thickness of a monolayer, but from potentials  $-1.35$  to  $-1$  V it has  $6.5$ – $7$  nm thickness, which corresponds to that of a bilayer. Contrary to the bilayer

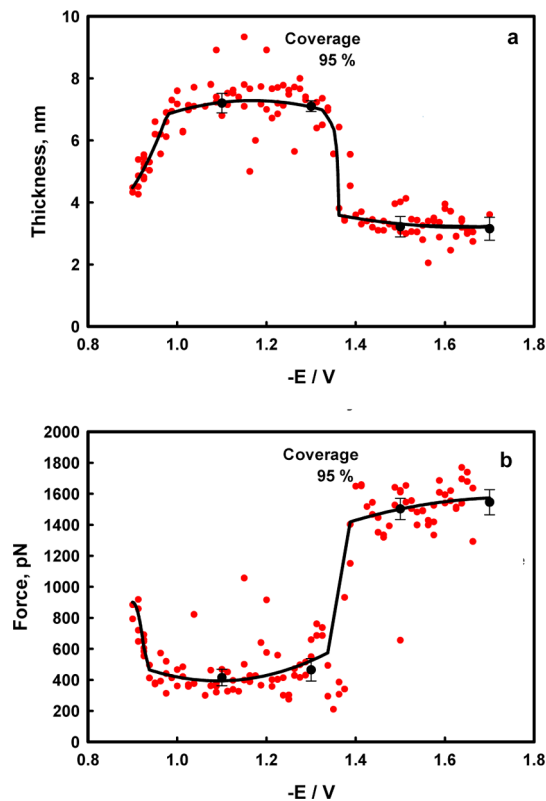


**Figure 4.** Coverage, (a) thickness, and (b) tip penetration force of DOPC bilayer on a Hg film electrode vs applied potential as measured by AFM. Each data point represents a single penetration event in a continuous series. The fit line is only a guide to the eye.

patch model, this presumed bilayer has significant resistance to penetration force (see Figure 4b) and shows  $95\%$  coverage. Under such conditions the existence of a near-continuous bilayer is indicated between potentials  $-1.35$  and  $-1.0$  V.

The monolayer/bilayer transition can be matched with the cathodic capacitance current peak at  $-1.4$  V on the RCV scan (peak 1 in Figure 2b). However the reversed peak 2 on the RCV anodic scan is considerably shifted to more positive potentials presumably due to the rapid voltage scanning. It is important to note that the bilayer is not stable when the electrode potential is taken to potentials more positive than  $-0.9$  V, where it reverts to a monolayer. For this reason the potential for deposition and monitoring is never brought to potentials more positive than  $-0.9$  V. Furthermore, the deposition of the bilayer as opposed to a monolayer is controlled by the applied potential and not the amount of DOPC in the vesicle dispersion.

The adsorption of the polar phospholipid heads onto the Hg surface when it is negatively polarized resulting in bilayer formation is consistent with physical chemical and thermodynamic theory. The surface free energy of the Hg/lipid interface decreases with increased negative potential<sup>27</sup> until it reaches that of the lipid polar heads when bilayer adsorption is favored. Indeed, one of the main properties of the Hg

electrode is that the Hg/electrolyte interface changes from an apolar surface (near the PZC) to a fairly polar surface having affinity for water at high positive or negative potentials. It is noted that this change in the Hg surface affinity of the water molecules is not due to a change in the intrinsic properties of the Hg, but is caused by the favorable orientation of the dipoles of the water molecules on Hg at higher electric field strengths. At these field strengths, bilayer adsorption on Hg is energetically favorable as previously simulated.<sup>31,33</sup> In addition to this, the increasing values of electric field applied across the phospholipid monolayer lead to the penetration of ions through the layer both simulated<sup>31</sup> and previously shown experimentally.<sup>27</sup> An accumulation of ions on the electrode surface between bilayer and electrolyte at negative field strengths has never been experimentally shown. The next step in this work is to study transport of electroactive ions across the patchy bilayer and continuous bilayer surface to the Hg surface. The technique of such study is described previously in Bizzotto's work.<sup>59</sup>

## CONCLUSIONS

1. A DOPC monolayer is deposited on Hg when the electrode is exposed to a  $5 \text{ mg cm}^{-3}$  DOPC vesicle dispersion, and its potential is scanned at  $40 \text{ V s}^{-1}$  between  $-0.4$  and  $-3.0 \text{ V}$ . The DOPC phospholipid monolayer is shown to have a thickness of  $2.5$ – $3 \text{ nm}$ , existing within a potential window of  $-0.2$  to  $-1.0 \text{ V}$ . At the following more negative applied potentials, the following structural changes in the monolayer have been characterized and are exactly coincident with the capacitance current discontinuities on the RCV plot.

$-1.1 \text{ V}$ : Sharp increase in thickness of the monolayer to  $4.6 \text{ nm}$ , corresponding to an ingress of water and cations and rearrangement of the monolayer to an ordered DOPC-electrolyte emulsion or more specifically a 2D lipid sponge.

$-1.2 \text{ V}$ : Sharp increase in thickness of the layer to  $6.3 \text{ nm}$ , corresponding to that of a bilayer. The coverage of  $65\%$  indicates that the Hg is covered in bilayer patches. This is in accord with the formation of bilayer patches from a monolayer.

$-1.4 \text{ V}$ : Sharp increase in thickness in the layer to  $8.6 \text{ nm}$  and further decrease in coverage to  $48\%$ . This indicates partial desorption of the bilayer patches to produce semivesicular structures on the Hg.

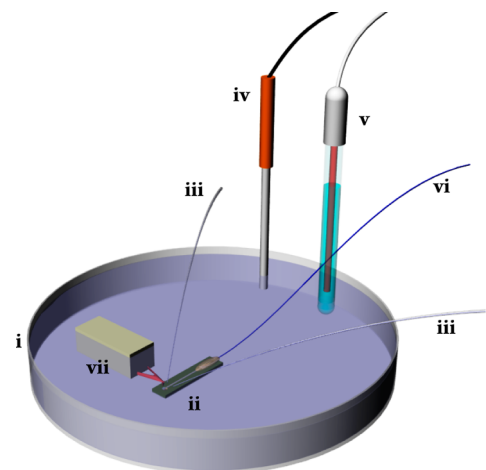


Figure 5. Schematic view of AFM setup: (i) a glass Petri dish, (ii) silicon wafer-based microfabricated Pt working electrodes, (iii) two glass capillaries, (iv) platinum counter electrode, (v) a reference electrode, (vi) insulated wire to Pt working electrode, and (vii) AFM tip.

$-1.5 \text{ V}$ : Layer thickness collapses to  $2.3 \text{ nm}$  with a coverage of  $95\%$ , indicative of monolayer formation at extreme negative potentials.

2. A near-continuous bilayer of thickness  $6.5$ – $7.0 \text{ nm}$  is deposited on the electrode exposed to a  $5 \text{ mg cm}^{-3}$  DOPC vesicle dispersion when the electrode potential is varied at  $40 \text{ V s}^{-1}$  from  $-1.1$  to  $-3.0 \text{ V}$ . This bilayer exists within a potential window from  $-1.0$  to  $-1.4 \text{ V}$  and reverts irreversibly to a monolayer at more positive potentials. In the RCV monitoring of the bilayer the electrode potential must therefore not be allowed to become more positive than  $-0.9 \text{ V}$ . At potentials more negative than  $-1.4 \text{ V}$  the bilayer reversibly converts to a layer of thickness  $2.3 \text{ nm}$  and coverage  $95\%$ . The formation of a phospholipid bilayer on Hg in aqueous electrolyte was previously considered unachievable. At negative potentials the Hg surface becomes effectively polar and would favor supporting a bilayer rather than a monolayer.<sup>33</sup>

3. The direct force microscopy characterization of structural changes of fluid lipid assemblies on Hg in an electric field has furthered an understanding of the molecular events underlying these changes. This has wide implications on the dependence of lipid–lipid and lipid–water interaction forces in the presence of an electric field and how these control the assembly of the lipid into different structures.

## MATERIALS AND METHODS

**Materials.** 1,2-Dioleoyl-*sn*-glycero-3-phosphocholine was obtained from Avanti Polar Lipids (Alabaster, USA) and was of  $>99\%$  purity. All other reagents were of analytical grade and purchased from SigmaAldrich.

**Methods. Electrochemical System Setup for Atomic Force Microscopy.** The system consisted of (i) a glass Petri dish, (ii) silicon wafer-based microfabricated Pt electrodes (Tyndall National

Institute, Ireland), (iii) two glass capillaries for  $0.1 \text{ mol dm}^{-3}$  KCl (capillary 1) and lipid dispersion in  $0.1 \text{ mol dm}^{-3}$  KCl (capillary 2) injection, respectively, (iv) a platinum counter electrode, and (v) a Ag/AgCl  $3.0 \text{ mol dm}^{-3}$  KCl reference electrode, REF201 Red Rod (VWR International Ltd.) (see Figure 5). All potentials in this paper unless otherwise stated are quoted *versus* the potential of this reference electrode. Silicon wafer-based microfabricated Pt electrodes were fixed to the Petri dish

with epoxy glue (Figure 5) and soldered with (vi) wire, and the wire contact was isolated by epoxy glue. The two glass capillaries (1 and 2) containing the electrolyte and the lipid dispersion, respectively, were fixed in position where the tapered thinnest end remained at a distance of 2–3 mm from the working electrode surface. The working electrode consisted of one Pt disk with a diameter of 1 mm embedded on a 28 by 3 mm<sup>2</sup> diced silicon wafer substrate possessing a surface of 0.2  $\mu\text{m}$  dry silicon oxide. Each Pt area was connected to respective contact pads by a 0.5 mm thick Pt trace interconnect, which was insulated with approximately 1.5 mm of  $\text{Si}_3\text{N}_4$  deposited by plasma-enhanced chemical vapor deposition (PECVD). The microfabricated Pt electrode was connected to a homemade potentiostat interfaced to a Powerlab 4/30 signal generator (AD Instruments Ltd.) controlled by Scope software.

**Electrode Pretreatment and RCV.** Electrodeposition of Hg onto Pt disk electrodes<sup>39,40,46,47</sup> was performed as previously reported but in a static cell. The working electrodes were cleaned prior to electrodeposition in a hot solution of a  $\text{H}_2\text{SO}_4$  (Fisher Scientific) and 30%  $\text{H}_2\text{O}_2$  (Fluka) mixture in a ratio of approximately 3:1, respectively, and rinsed with Milli-Q 18.2M $\Omega$  (Millipore UK) water before drying under nitrogen ( $\text{N}_2$ ). The reduction of Hg onto the Pt disk was performed at −0.4 V and monitored by means of chronocoulometry with a cutoff value for the charge ( $Q$ ) flowed of <1 C per electrode in 50 mmol dm<sup>−3</sup>  $\text{Hg}(\text{NO}_3)_2$  solution. Once the designated amount of charge had passed, the circuit was opened and the electrode was washed by constant flow of 5 cm<sup>3</sup> min<sup>−1</sup> of Milli-Q 18.2M $\Omega$  (Millipore UK) water for 30 min. The Pt electrodes with electrodeposited Hg are subsequently referred to as Pt/Hg electrodes. Rapid cyclic voltammetry as the electrochemical treatment and monitoring technique was carried out in 0.1 mol dm<sup>−3</sup> KCl (calcined before solvation at 600 °C) at room temperature.

**Electrochemical Preparation and DOPC Deposition for AFM Experiment.** The electrochemical “cell” was filled with 0.1 mol dm<sup>−3</sup> KCl solution, the electrodes were connected to the potentiostat, and each of two capillaries (1 and 2) were filled with (1) 0.1 mol dm<sup>−3</sup> KCl solution and (2) 5 mg cm<sup>−3</sup> DOPC dispersion, in 0.1 mol dm<sup>−3</sup> KCl. DOPC dispersion was prepared by shaking dry DOPC with 0.1 mol dm<sup>−3</sup> KCl solution. DOPC dispersion was used that would successfully cover the electrode with a monolayer. A 5 mg cm<sup>−3</sup> DOPC concentration was chosen because a presumed bilayer formation necessitated a minimum DOPC concentration of 4 mg cm<sup>−3</sup>. Clear contact of the electrode with a considerable excess of DOPC was required to promote bilayer deposition. RCV at scan rates of 40 V s<sup>−1</sup> was initiated continuously at a voltage excursion from −0.4 to −3 V in order to clean the Pt/Hg electrode; 10–20 mm<sup>3</sup> of lipid dispersion in 0.1 mol dm<sup>−3</sup> KCl was injected slowly into the cell from capillary 2 until the lipid dispersion covered the Pt/Hg electrode. For monolayer preparation RCV at scan rates of 40 V s<sup>−1</sup> with a voltage excursion from −0.4 to −3 V was then applied for 10–20 s to facilitate a coating of the electrode as done previously.<sup>39,40,46,47</sup> Subsequently the lipid dispersion was flushed with 0.1 mol dm<sup>−3</sup> KCl solution from capillary 1, and RCV at scan rates of 40 V s<sup>−1</sup> with a voltage excursion from −0.4 to −1.7 V was initiated until stable capacitance current peaks appeared. For presumed bilayer formation RCV at scan rates of 40 V s<sup>−1</sup> with a voltage excursion from −1.1 to −3 V was applied for 10–20 s to facilitate a coating of the electrode. Subsequently the lipid dispersion was flushed with 0.1 mol dm<sup>−3</sup> KCl solution from capillary 1, and RCV at scan rates of 40 V s<sup>−1</sup> with a voltage excursion from −1.7 to −0.9 V was initiated until stable presumed bilayer capacitance current peaks appeared. Subsequently, in order to electrochemically characterize the lipid-coated and uncoated electrodes, RCV voltage excursions from −0.4 V to −1.7 V were applied to the monolayer-coated/uncoated Pt/Hg (Figure 2a) and from −1.7 to −0.9 V to the bilayer-coated/uncoated Pt/Hg (Figure 2b) at scan rates of 40 V s<sup>−1</sup>.

**Atomic Force Microscopy.** AFM curves were obtained using a Dimension 3100 AFM (Bruker) with a Direct Drive Tapping cantilever holder for fluid operation. Repeated force scans on the Pt/Hg electrode surface were obtained by vertically ramping a nonconductive silicon nitride tip (Bruker, model MLCT) at

different surface locations while recording the AFM cantilever deflection as a function of the relative tip–sample distance, according to standard procedures.<sup>60,61</sup> The cantilever spring constant was measured in air as  $0.026 \pm 0.001 \text{ N m}^{-1}$  using the thermal tune function on a Multimode 8 AFM (Bruker). Prior to the experiment the probe was treated with aqua regia for 30 s in order to remove traces of gold, which can amalgamate with mercury. Subsequently it was washed with water, dried, and treated with dichlorodimethylsilane for 30 s. The silanization routine was found operationally to give reproducible force–distance curves presumably because it prevented the lipid from adhering to the tip. The reason for this is being investigated and will be reported in a subsequent paper. The electrode was mounted on the AFM stage using the electrochemical system setup for AFM experiment (see the Electrochemical System Setup section), and electrochemical preparation was performed according to the procedure described in the Electrochemical Preparation section above. A deflection sensitivity calibration was carried out by performing a force–distance curve on the hard silicon surrounding the Pt/Hg electrode prior to each experimental run. The mercury electrode was located and the AFM probe positioned precisely at the apex of the mercury electrode using the motorized stage and top-down CCD microscope of the Dimension 3100. Following this, force–distance experiments using the AFM tip were carried out at different potentials. All experiments were carried out using two separate procedures. In the first procedure, the potential was fixed at −0.25, −0.45, −0.65, −0.85, −1.05, −1.25, −1.45, −1.65, and −1.85 V for the “monolayer” experiment and at −1.7, −1.5, −1.3, and −1.1 V for the “bilayer” experiment. Subsequently 50–100 force–distance curves were measured at each of these potentials. In the second procedure, the force–distance experiments were carried out continuously while the potential was very slowly varied from −0.2 V to −1.8 V and back for the monolayer experiment and from −1.7 V to −0.9 V and back for the bilayer experiment. The existence of a lipid layer coating on the Hg showed up as a penetration step on the force–distance curve. The thickness and penetration force of the lipid layers were determined as the position of the penetration step on the distance axis and on the force axis, respectively, of the force–distance curve. The quoted “phospholipid layer coverage” was operationally defined as the percentage of curves with a defined tip penetration step out of the total quantity of measured curves. For example from 100 curves produced for a monolayer at −1.25 V, 65 of them did not have a DOPC layer penetration step and 35 of them did have a step. This coverage estimation assumed that the DOPC assemblies on Hg are mobile so that each penetration is a random test of the monolayer structure at that point in time.

In a raw force curve (deflection vs distance) the x axis is in nanometers and represents the piezoelectric displacement, *i.e.*, the distance traveled by the sample toward or away from the tip. Piezo displacement was transformed into tip–sample separation, by adding the cantilever deflection. The latter is given in voltage in the original force curve and was rescaled into nanometers by multiplying by the deflection sensitivity factor (in nm V<sup>−1</sup>). When the tip is deflected against a hard surface, the deflection sensitivity corresponds to the inverse of the slope of the linear region of the force curve (the contact part). The deflection sensitivity obtained on the hard silicon surround was used to rescale correctly the curves performed on Hg. After this procedure the contact part of the force curve was transformed into a vertical line for hard surfaces. If the surface is compliant, the contact part is curved, and negative distances correspond to indentation, *i.e.*, to the deformation of the surface.

**Conflict of Interest:** The authors declare no competing financial interest.

**Acknowledgment.** M.G. was supported during his stay in Leeds by an EU grant Student Mobility for Placements–Erasmus awarded by Università degli Studi di Milano. A.V. was supported by the UK Royal Society Brian Mercer Award during the time that he completed this work. Equipment and consumables were funded by EPSRC grant numbers EP/G015325/1 and EP/017566/1. A.V. expresses thanks to Zachary Coldrick (previously

of CMNS, School of Chemistry, University of Leeds, UK) for helpful discussions.

## REFERENCES AND NOTES

- Volinsky, R.; Kliger, M.; Sheynis, T.; Kolusheva, S.; Jelinek, R. Glass-Supported Lipid/Polydiacetylene Films for Colour Sensing of Membrane-Active Compounds. *Biosens. Bioelectron.* **2007**, *22*, 3247–3251.
- Cush, R.; Cronin, J. M.; Stewart, W. J.; Maule, C. H.; Molloy, J.; Goddard, N. J. The Resonant Mirror: A Novel Optical Biosensor for Direct Sensing of Biomolecular Interactions Part I: Principle of Operation and Associated Instrumentation. *Biosens. Bioelectron.* **1993**, *8*, 347–354.
- Girard-Egrot, A. P.; Marquette, C. A.; Blum, L. J. Biomimetic Membranes and Biomolecule Immobilisation Strategies for Nanobiotechnology Applications. *Int. J. Nanotechnol.* **2010**, *7*, 753–780.
- Reimhult, E.; Kumar, K. Membrane Biosensor Platforms Using Nano and Microporous Supports. *Trends Biotechnol.* **2008**, *26*, 82–89.
- Richter, R. P.; Berat, R.; Brisson, A. R. Formation of Solid-Supported Lipid Bilayers: An Integrated View. *Langmuir* **2006**, *22*, 3497–3505.
- Rossi, C.; Chopineau, J. Biomimetic Tethered Lipid Membranes Designed for Membrane-Protein Interaction Studies. *Eur. Biophys. J.* **2007**, *36*, 955–965.
- Leblanc, R. M. Molecular Recognition at Langmuir Monolayers. *Curr. Opin. Chem. Biol.* **2006**, *10*, 529–536.
- Park, J.; Kurosawa, S.; Takai, M.; Ishihara, K. Antibody Immobilization to Phospholipid Polymer Layer on Gold Substrate of Quartz Crystal Microbalance Immunosensor. *Colloids Surf., B* **2007**, *55*, 164–172.
- Li, J.; Ding, L.; Wang, E.; Dong, S. The Ion Selectivity of Monensin Incorporated Phospholipid/Alkanethiol Bilayers. *J. Electroanal. Chem.* **1996**, *414*, 17–21.
- Ding, L.; Li, J.; Wang, E.; Dong, S. K<sup>+</sup> Sensors Based on Supported Alkanethiol/Phospholipid Bilayers. *Thin Solid Films* **1997**, *293*, 153–158.
- Cannes, C.; Kanoufi, F.; Bard, A. J. Cyclic Voltammetry and Scanning Electrochemical Microscopy of Ferrocenemethanol at Monolayer and Bilayer-Modified Gold Electrodes. *J. Electroanal. Chem.* **2003**, *547*, 83–91.
- Zawisza, I.; Bin, X.; Lipkowski, J. Spectroelectrochemical Studies of Bilayers of Phospholipids in Gel and Liquid State on Au(111) Electrode Surface. *Bioelectrochemistry* **2004**, *63*, 137–147.
- Burgess, I.; Li, M.; Horswell, S. L.; Szymanski, G.; Lipkowski, J.; Majewski, J.; Satija, S. Electric Field-Driven Transformations of a Supported Model Biological Membrane—An Electrochemical and Neutron Reflectivity Study. *Biophys. J.* **2004**, *86*, 1763–1776.
- Lipkowski, J. Building Biomimetic Membrane at a Gold Electrode Surface. *Phys. Chem. Chem. Phys.* **2010**, *12*, 13874–13887.
- Burgess, I.; Li, M.; Horswell, S. L.; Szymanski, G.; Lipkowski, J.; Satija, S.; Majewski, J. Influence of the Electric Field on a Bio-Mimetic Film Supported on a Gold Electrode. *Colloids Surf., B* **2005**, *40*, 117–122.
- Krysinski, P.; Moncelli, M. R.; Tadini-Buoninsegni, F. A Voltammetric Study of Monolayers and Bilayers Self-Assembled on Metal Electrodes. *Electrochim. Acta* **2000**, *45*, 1885–1892.
- Chen, M.; Li, M.; Brosseau, C. L.; Lipkowski, J. AFM Studies of Effects of Temperature and Electric Field on the Structure of a DMPC-Cholesterol Bilayer Supported on a Au(111) Electrode Surface. *Langmuir* **2009**, *25*, 1028–1037.
- Li, M.; Chen, M.; Sheepwash, E.; Brosseau, C. L.; Li, H.; Pettinger, B.; Gruler, H.; Lipkowski, J. AFM Studies of Solid-Supported Lipid Bilayers Formed at a Au(111) Electrode Surface Using Vesicle Fusion and a Combination of Langmuir-Blodgett and Langmuir-Schaefer Techniques. *Langmuir* **2008**, *24*, 10313–10323.
- Kycia, A. H.; Wang, J.; Merrill, R.; Lipkowski, J. Atomic Force Microscopy Studies of a Floating-Bilayer Lipid Membrane on a Au(111) Surface Modified with a Hydrophilic Monolayer. *Langmuir* **2011**, *27*, 10867–10877.
- Miller, I. R. Charge transport in lipid layers and in biological membranes. In *Topics in Bioelectrochemistry and Bioenergetics*; Milazzo, G., Ed.; John Wiley and Sons: Chichester, 1981; Vol. 4, pp 161–224.
- Nelson, A.; Benton, A. Phospholipid Monolayers at the Mercury/Water Interface. *J. Electroanal. Chem.* **1986**, *202*, 253–270.
- Nelson, A.; Auffret, N. Phospholipid Monolayers of Doleoyl Lecithin at the Mercury/Water Interface. *J. Electroanal. Chem.* **1988**, *244*, 99–113.
- Nelson, A.; Auffret, N. Phospholipid Monolayers of Di-Oleoyl Lecithin (Di-O-PC) at the Mercury Water Interface. Effect on Faradaic Reactions. *J. Electroanal. Chem.* **1988**, *248*, 167–180.
- Nelson, A. Electrochemistry of Mercury Supported Phospholipid Monolayers and Bilayers. *Curr. Opin. Colloid Interface Sci.* **2010**, *15*, 455–466.
- Whitehouse, C.; O'Flanagan, R.; Lindholm-Sethson, B.; Movaghah, B.; Nelson, A. Application of Electrochemical Impedance Spectroscopy to the Study of Doleoyl Phosphatidylcholine Monolayers on Mercury. *Langmuir* **2004**, *20*, 136–144.
- Chen, S.; Abruna, H. D. Electrode Potential Induced Reorientation of a Phospholipid Monolayer on a Mercury Electrode Surface. *Langmuir* **1994**, *10*, 3343–3349.
- Bizzotto, D.; Nelson, A. Continuing Electrochemical Studies of Phospholipid Monolayers of Doleoyl Phosphatidylcholine at the Mercury–Electrolyte Interface. *Langmuir* **1998**, *14*, 6269–6273.
- Bizzotto, D.; Yang, Y.; Shepherd, J. L.; Stoodley, R.; Agak, J.; Stauffer, V.; Lathuilliere, M.; Akhtar, A. S.; Chung, E. Electrochemical and Spectroelectrochemical Characterization of Lipid Organization in an Electric Field. *J. Electroanal. Chem.* **2004**, *574*, 167–184.
- Stoodley, R.; Bizzotto, D. Epi-Fluorescence Microscopic Characterization of Potential-Induced Changes in a DOPC Monolayer on a Hg Drop. *Analyst* **2003**, *128*, 552–561.
- Nelson, A.; Bizzotto, D. Chronoamperometric Study of Tl(I) Reduction at Gramicidin-Modified Phospholipid-Coated Mercury Electrodes. *Langmuir* **1999**, *15*, 7031–7039.
- Brukhno, A. V.; Akinshina, A.; Coldrick, Z.; Nelson, A.; Auer, S. Phase Phenomena in Supported Lipid Films under Varying Electric Potential. *Soft Matter* **2011**, *7*, 1006–1017.
- Nelson, A. Electrochemical Analysis of a Phospholipid Phase Transition, Journal of Electroanalytical Chemistry. *J. Electroanal. Chem.* **2007**, *601*, 83–93.
- Leermakers, F. A. M.; Nelson, A. Substrate-Induced Structural Changes in Electrode-Adsorbed Lipid Layers: A Self-Consistent Field Theory. *J. Electroanal. Chem.* **1990**, *278*, 53–72.
- DeNardis, N. I.; Žutić, V.; Svetličić, V.; Frkanec, R. Adhesion Signals of Phospholipid Vesicles at an Electrified Interface. *J. Membr. Biol.* **2012**, *245*, 573–582.
- Nelson, A.; Leermakers, F. A. M. Substrate-Induced Structural Changes in Electrode-Adsorbed Lipid Layers: Experimental Evidence from the Behaviour of Phospholipid Layers on the Mercury-Water Interface. *J. Electroanal. Chem.* **1990**, *278*, 73–83.
- Monné, J.; Díez, Y.; Puy, J.; Galceran, J.; Nelson, A. Interpreting Ion Fluxes to Channel Arrays in Monolayers. *Langmuir* **2007**, *23*, 10581–10588.
- Nelson, A. Conducting Gramicidin Channel Activity in Phospholipid Monolayers. *Biophys. J.* **2001**, *80*, 2694–2703.
- Mauzeroll, J.; Buda, M.; Bard, A. J.; Prieto, F.; Rueda, M. Detection of Tl(I) Transport through a Gramicidin–Doleoylphosphatidylcholine Monolayer Using the Substrate Generation–Tip Collection Mode of Scanning Electrochemical Microscopy. *Langmuir* **2002**, *18*, 9453–9461.
- Coldrick, Z.; Steenson, P.; Millner, P.; Davies, M.; Nelson, A. Phospholipid Monolayer Coated Microfabricated Electrodes to Model the Interaction of Molecules with Biomembranes. *Electrochim. Acta* **2009**, *54*, 4954–4962.

40. Coldrick, Z.; Penezic, A.; Gasparovic, B.; Steenson, P.; Merrifield, J.; Nelson, A. High Throughput Systems for Screening Biomembrane Interactions on Fabricated Mercury Film Electrodes. *J. Appl. Electrochem.* **2011**, *41*, 939–949.

41. Agak, J. O.; Stoodley, R.; Retter, U.; Bizzotto, D. On The Impedance of a Lipid-Modified Hg | Electrolyte Interface. *J. Electroanal. Chem.* **2004**, *562*, 135–144.

42. Gao, X.; White, H. S.; Chen, S.; Abruna, H. D. Electric-Field-Induced Transitions of Amphiphilic Layers on Mercury Electrodes. *Langmuir* **1996**, *11*, 4554–4563.

43. Hernández, V. A.; Lendeckel, U.; Scholz, F. Electrochemistry of Adhesion and Spreading of Lipid Vesicles on Electrodes. *Mod. Aspects Electrochem.* **2013**, *56*, 189–247.

44. Herrero, R.; Barriada, J. L.; López-Fonseca, J. M.; Moncelli, M. R.; Sastre de Vicente, M. E. Effect of Ionic Strength on the Electrochemical Behavior of Glutathione on a Phospholipid Self-Assembled Monolayer on Mercury. *Langmuir* **2000**, *16*, 5148–5153.

45. Rueda, M.; Navarro, I.; Ramirez, G.; Prieto, F.; Nelson, A. Impedance Measurements with Phospholipid-Coated Mercury Electrodes. *J. Electroanal. Chem.* **1998**, *454*, 155–160.

46. Ormategui, N.; Zhang, S.; Loinaz, I.; Brydson, R.; Nelson, A.; Vakurov, A. Interaction of Poly(N-isopropylacrylamide) (pNIPAM) Based Nanoparticles and Their Linear Polymer Precursor with Phospholipid Membrane Models. *Bioelectrochemistry* **2012**, *87*, 211–219.

47. Vakurov, A.; Brydson, R.; Nelson, A. Electrochemical Modeling of the Silica Nanoparticle–Biomembrane Interaction. *Langmuir* **2012**, *28*, 1246–1255.

48. Roelfs, B.; Bunge, E.; Schröter, C.; Solomon, T.; Meyer, H.; Nichols, R. J.; Baumgärtel, H. Adsorption of Thymine on Gold Single-Crystal Electrodes. *J. Phys. Chem. B* **1997**, *101*, 754–765.

49. Stamou, D.; Gourdon, D.; Liley, M.; Burnham, N. A.; Kulik, A.; Vogel, H.; Duschl, C. Uniformly Flat Gold Surfaces: Imaging the Domain Structure of Organic Monolayers Using Scanning Force Microscopy. *Langmuir* **1997**, *13*, 2425–2428.

50. Silva, F.; Martins, A. Surface Reconstruction of Gold Single Crystals: Electrochemical Evidence of the Effect of Adsorbed Anions and Influence of Steps and Terraces. *Electrochim. Acta* **1998**, *44*, 919–929.

51. Hwang, J.; Tamm, L. K.; Böhm, C.; Ramalingam, T. S.; Betzig, E.; Edidin, M. Nanoscale Complexity of Phospholipid Monolayers Investigated by Near-Field Scanning Optical Microscopy. *Science* **1995**, *270*, 610–614.

52. Lewis, B. A.; Engelman, D. M. Lipid Bilayer Thickness Varies Linearly with Acyl Chain Length in Fluid Phosphatidylcholine Vesicles. *J. Mol. Biol.* **1983**, *166*, 211–217.

53. King, G. I.; White, S. H. Determining Bilayer Hydrocarbon Thickness from Neutron Diffraction Measurements Using Strip-Function Models. *Biophys. J.* **1986**, *49*, 1047–1054.

54. Nagle, J. F.; Tristram-Nagle, S. Structure of Lipid Bilayers. *Biochim. Biophys. Acta* **2000**, *1469*, 159–95.

55. Uhrikova, D.; Balgavy, P.; Kucerka, N.; Islamov, A.; Gordeliy, V.; Kuklin, A. Small-Angle Neutron Scattering Study of the n-Decane Effect on the Bilayer Thickness in Extruded Unilamellar Dioleoylphosphatidylcholine Liposomes. *Biophys. Chem.* **2000**, *165*–170.

56. Hristova, K.; White, S. H. Determination of the Hydrocarbon Core Structure of Fluid Dioleoylphosphocholine (DOPC) Bilayers by X-Ray Diffraction Using Specific Bromination of the Double-Bonds: Effect of Hydration. *Biophys. J.* **1998**, *74*, 2419–2433.

57. Tahara, Y.; Fujiyoshi, Y. A New Method to Measure Bilayer Thickness: Cryo-Electron Microscopy of Frozen Hydrated Liposomes and Image Simulation. *Micron* **1994**, *25*, 141–149.

58. Barauskas, J.; Johnsson, M.; Tiberg, F. Self-Assembled Lipid Superstructures: Beyond Vesicles and Liposomes. *Nano Lett.* **2005**, *5*, 1615–1619.

59. Bizzotto, D.; McAlees, A.; Lipkowski, J.; McCrindle, R. Barrier Properties of a Thin Film of 4-Pentadecylpyridine Coated at Au(111) Electrode Surface. *Langmuir* **1995**, *11*, 3243–3250.

60. Cappella, B.; Dietler, G. Force-Distance Curves by Atomic Force Microscopy. *Surf. Sci. Rep.* **1999**, *34*, 1–104.

61. Butt, H. J.; Cappella, B.; Kappl, M. Force Measurements with the Atomic Force Microscope: Technique, Interpretation and Applications. *Surf. Sci. Rep.* **2005**, *59*, 1–152.